CORE
Metadata, citation and similar papers at core.ac.uk
Provided by University of Southern Denmark Research Output

First published September 30, 2009; doi:10.1152/ajpregu.00321.2009.

Prostasin-dependent activation of epithelial Na^+ channels by low plasmin concentrations

Per Svenningsen,[1] Torben R. Uhrenholt,[1] Yaseelan Palarasah,[2] Karsten Skjødt,[2] Boye L. Jensen,[1] and Ole Skøtt[1]

Departments of [1]Physiology and Pharmacology and [2]Immunology and Microbiology, Institute of Medical Biology, University of Southern Denmark, Odense, Denmark

Submitted 9 June 2009; accepted in final form 29 September 2009

Svenningsen P, Uhrenholt TR, Palarasah Y, Skjødt K, Jensen BL, Skøtt O. Prostasin-dependent activation of epithelial Na^+ channels by low plasmin concentrations. *Am J Physiol Regul Integr Comp Physiol* 297: R1733–R1741, 2009. First published September 30, 2009; doi:10.1152/ajpregu.00321.2009.—Several pathophysiological conditions, including nephrotic syndrome, are characterized by increased renal activity of the epithelial Na^+ channel (ENaC). We recently identified plasmin in nephrotic urine as a stimulator of ENaC activity and undertook this study to investigate the mechanism by which plasmin stimulates ENaC activity. Cy3-labeled plasmin was found to bind to the surface of the mouse cortical collecting duct cell line, M-1. Binding depended on a glycosylphosphatidylinositol (GPI)-anchored protein. Biotin-label transfer showed that plasmin interacted with the GPI-anchored protein prostasin on M-1 cells and that plasmin cleaved prostasin. Prostasin activates ENaC by cleavage of the γ-subunit, which releases an inhibitory peptide from the extracellular domain. Removal of GPI-anchored proteins from the M-1 cells with phosphatidylinositol-specific phospholipase C (PI-PLC) inhibited plasmin-stimulated ENaC current in monolayers of M-1 cells at low plasmin concentration (1–4 μg/ml). At a high plasmin concentration of 30 μg/ml, there was no difference between cell layers treated with or without PI-PLC. Knockdown of prostasin attenuated binding of plasmin to M1 cells and blocked plasmin-stimulated ENaC current in single M-1 cells, as measured by whole-cell patch clamp. In M-1 cells expressing heterologous FLAG-tagged prostasin, γENaC and prostasin were colocalized. A monoclonal antibody directed against the inhibitory peptide of γENaC produced specific immunofluorescence labeling of M-1 cells. Pretreatment with plasmin abolished labeling of M-1 cells in a prostasin-dependent way. We conclude that, at low concentrations, plasmin interacts with GPI-anchored prostasin, which leads to cleavage of the γ-subunit and activation of ENaC, while at higher concentrations, plasmin directly activates ENaC.

serine protease; sodium retention; kidney; M-1 cells; nephrotic syndrome

IN THE ALDOSTERONE-RESPONSIVE epithelial cells of kidney, the epithelial sodium channel (ENaC) establishes the rate-limiting step in transepithelial sodium transport, which is of critical importance in the control of sodium balance, blood volume, and blood pressure (45). The channel is composed of three homologous subunits α, β, γ, (8), and each subunit has intracellular N- and C-termini, two transmembrane domains, and a large extracellular domain (18). The activity of ENaC is regulated by hormones, e.g., aldosterone (2, 28, 30) and vasopressin (13), and local factors, e.g., sodium concentration, pH, and intracellular Ca^{2+} (34). Moreover, within the last decade serine proteases have also been shown to activate ENaC (42). Serine proteases comprise a large family of proteolytic enzymes that are involved in a plethora of physiological and pathophysiological functions, ranging from digestive proteases that break down food proteins to proteases that recognize specific cleavage sites (20). The exact mechanism by which serine protease activates ENaC is still not resolved (37); however, cleavage of the extracellular domain of the α and γ subunit seems to be a critical step in the proteolytic activation of ENaC (24, 36). The cleavages of the extracellular domain may lead to release of an inhibitory peptide and an increase in the open-probability (5, 24). A fraction of the ENaC subunits are cleaved within the biosynthesis pathway by the intracellular protease furin (22, 23), giving rise to both noncleaved and cleaved ENaC channels in the plasma membrane (23). Thus, at the plasma membrane, a pool of noncleaved channels are present, which can be activated by extracellular serine proteases (1, 6, 7, 11, 42, 43). Several extracellular serine proteases have been shown to activate ENaC in vitro through cleavage of the γ subunit, including channel activating protease 1 (CAP1/prostasin) (42), trypsin (42), chymotrypsin (11), neutrophil elastase (6), and plasmin (35, 41) with prostasin as the relevant candidate under physiological conditions (46). Moreover, proteolytic ENaC activation may be a means of regulating sodium reabsorption in kidney in vivo, since rats fed a 1% sodium diet express both full-length and cleaved γENaC at the plasma membrane, while Na-depleted or aldosterone-treated rats mainly express the cleaved subunit (16).

We recently identified the serine protease plasmin as an ENaC activator in urine from rats and humans with nephrotic syndrome (41). Plasmin-stimulated ENaC activity could contribute to the observed renin-angiotensin-aldosterone independent primary sodium retention characteristic for the disease. Plasmin was shown to stimulate ENaC activity in expression systems and in collecting duct cells, as well as to cleave purified γ-subunit (35, 41), leading to the release of an inhibitory peptide from the extracellular domain (41). Thus, this study was undertaken to investigate potential interaction targets and mechanisms by which plasmin stimulates ENaC activity in the collecting duct cell line M-1.

MATERIALS AND METHODS

Cell culture. M-1 cells were obtained from American Type Culture Collection (Boras, Sweden) and grown in 25-cm^2 flasks (Nunc, Roskilde, Denmark) until confluence. The medium was DMEM:F12 (Life Technologies, Tåstrup, Denmark) supplemented with 5% FCS (Life Technologies) and 5 μM dexamethasone (Sigma, Broendby, Denmark), and cells were kept at 37°C in 5% CO_2.

Address for reprint requests and other correspondence: B. L. Jensen, Physiology and Pharmacology, Institute of Medical Biology, Univ. of Southern Denmark, Winslowparken 21; DK-5000 Odense C. (e-mail: bljensen@health.sdu.dk).

0363-6119/09 $8.00 Copyright © 2009 the American Physiological Society

Downloaded from http://ajpregu.physiology.org/ by 10.220.33.1 on January 14, 2017

Biotin-label transfer experiment. Interaction partners of plasmin were identified using ProFound Sulfo-SBED Biotin Label Transfer kit (Pierce, Herlev, Denmark), as described by the manufacturer. Briefly, plasmin was labeled with the biotinylated cross-linker sulfo-SBED. Labeled plasmin was added to confluent M-1 cells grown in six-well plates (Nunc) and incubated for 5 min at 37°C in 5% CO_2. The cross-linker was activated by UV-illumination for 15 min with cells incubated on ice. Cells were lysed and biotinylated proteins were precipitated with streptavidin-agarose. The pelleted proteins were reduced and analyzed by immunoblotting.

siRNA-mediated knockdown. M-1 cells were transfected with siRNA using DharmaFECT1 (Dharmacon, Herlev, Denmark), as previously described (41). Prostasin was knocked down using 50 nM ON-TARGET plus PRSS8 siRNA (cat. no. L-053718-01, Dharmacon). For negative control, cells were transfected with Silencer Negative Control (cat. no. AM4611, Ambion, Naerum, Denmark).

PI-PLC was purchased from Invitrogen and used at a concentration of 0.1 U/ml for at least 60 min prior to experiments. Recombinant GST-tagged prostasin was purchased from Abnova (Taiwan), and prostasin cleavages were assayed as described previously (32).

Reverse transcriptase-quantitative PCR. RNA was extracted from M-1 cells in accordance with the manufacturer's instructions (Qiagen Mini Kit, Qiagen, Ballerup, Denmark) and reverse transcribed using iScript cDNA synthesis kit (Bio-Rad, Copenhagen, Denmark). Prostasin cDNA levels were measured using mouse prostasin primers. Prostasin cDNA levels were normalized to 18S cDNA. All reactions were run with IQ SYBR Green Supermix (Bio-Rad) on an Mx3000P (Stratagene, La Jolla, CA) thermocycler.

Urine from rats with puromycin aminonucleoside-induced nephrotic syndrome. Puromycin aminonucleoside (PAN) nephrosis in rats was induced, and urine was collected, as previously described (3, 41). The experiments were approved by the Danish Animal Experiments Inspectorate under the Department of Justice (171001-096).

Whole-cell patch clamp of single M-1 cells. Whole-cell patch clamp was carried out as previously described (41). Briefly, M-1 cells were seeded onto coverslips and incubated at 37°C in 5% CO_2. Patch-clamp experiments were conducted on single M-1 cells 24–48 h after seeding the cells. Current was monitored by the response to a voltage step to −150 mV for 200 ms from a holding potential of −60 mV, which was repeated every second. The effect of rat plasmin (10 μg/ml, Innovative Research, Novi, MI) was tested by dissolving in bath solution and applying the sample by a pipette upstream of the single M-1 cell with the solution containing plasmin.

Ussing chamber experiments. M-1 cells were grown on 1.12-cm^2 filter supports (Corning, Brondby, Denmark) for 10–14 days and mounted in a Ussing chamber (Physiologic Instruments, San Diego, CA), bathed in saline solution containing: [in mmol/l: 116 NaCl, 24 $NaHCO_3$, 4 KCl, 1 $MgCl_2$, 1 $CaCl_2$, 5 glucose], as described previously (41). The bath solution was kept at 37°C and continuously bubbled with 5% CO_2 in air to keep pH at 7.4 and assure stirring. To minimize ENaC activation by endogenous proteases, the confluent M-1 cells grown on filters were preincubated overnight with the furin inhibitor dec-RVKR-cmk (decanoyl-Arg-Val-Lys-Arg-chloromethyl ketone from BioMol/SMS-gruppen, Rungsted Kyst, Denmark) before experiments. The effect of the different plasmin concentrations was tested by monitoring the current induced by addition to the apical bath of plasmin. Subsequently, trypsin (100 μg/ml; Sigma) was added to measure the maximal serine protease activatable ENaC activity. To assess the involvement of glucosylphosphatidylinositol (GPI)-anchored proteins, monolayers were treated with or without 0.1 U/ml PI-PLC (Invitrogen, Tåstrup, Denmark) for at least 1 h before experiments. The amiloride-sensitive current was determined by adding amiloride at a final concentration of 100 μM to the apical bath at the end of the experiment.

Laser-scanning confocal microscopy with plasmin-Cy3. The fluorophore Cy3 (Amersham Biosciences, Hillerod, Denmark) was coupled to rat plasmin (Innovative Research) according to the manufacturer's protocol. For imaging plasmin-Cy3 dynamics, plasmin-Cy3 in DMEM:F12 (Invitrogen) was superfused to bind on M-1 cell surface. Confocal laser-scanning fluorescence microscopy (Olympus FV1000, Hamburg, Germany) was performed using a ×20 (numerical aperture, 0.5) Olympus water immersion objective. The scanning area was set to 512 × 512 pixels with and without internal zoom. Full-frame imaging was performed at 1 Hz using excitation from a laser at 559 nm with fluorescence monitored through a 570–670 nm bandpass [Acousto-optic tunable filter (AOTF)]. Laser power was adjusted (transmissivity 8%; photomultiplier tube voltage 450–550 V) to obtain images with a mean intensity of 150 arbitrary intensity units (range 100–4,095). This ensured fluorescence acquisition over the full dynamic range of Plasmin-Cy3 without pixel saturation or excessive photobleaching.

Generation and purification of monoclonal antibodies. To test the cleavage of the γENaC subunit, we developed a monoclonal antibody against the inhibitory peptide from the human γENaC subunit (Acc. Num: NM_001039) corresponding to amino acid residue 139–160. The peptide [EAESWNSVSEGKQPRFSHRIPLC] was synthesized (EzBiolab, Carmel, IN) with an extra C-terminal cysteine to facilitate conjugation to tuberculin-purified protein derivative. BALB/c×NMRI mice were immunized subcutaneously three times with 25 μg the peptide adsorbed to $Al(OH)_3$, mixed in 1:1 ratio with Freunds incomplete adjuvant. Four days prior to the fusion, the mice received an intravenous injection with 25 μg antigen administered with adrenalin. The fusion and selection were done essentially as described by Köhler and Milstein (26). The SP2/0-AG14 myeloma cell line was used as a fusion partner. Positive clones were selected by differential screening against the peptide in ELISA. Cloning was performed by limited dilution. Single clones were grown in culture flasks in RPMI+10% FCS, and mAbs were purified from culture supernatant by protein A affinity chromatography using the äkta FPLC system, according to the manufacturer's instructions (Amersham Pharmacia, Uppsala, Sweden).

Immunocytofluorescence. To test whether prostasin and γENaC are colocalized, M-1 cells were grown on coverslips and transfected with a plasmid expressing C-terminal FLAG-tagged human prostasin (Origene, Rockville, MD) using Lipofectamine LTX (Invitrogen), according to the manufacturer's instructions. Twenty-four hours after transfection, the cells were fixed in 4% formaldehyde/PBS, washed with PBS-Tween (PBST), and incubated with antibodies against the mouse FLAG-tag (Sigma) and rabbit polyclonal γENaC antibody (Sigma) for 1 h at room temperature. We used the Duolink proximity ligation assay (Olink Bioscience, Uppsala, Sweden), according to the manufacturer's instructions to test if prostasin and γENaC is colocalized. To visualize punctate signals, intensity was enhanced post hoc (Fig. 4*A*) using Adobe Photoshop CS4. Furthermore, we tested the colocalization using standard immunofluorescence, where the primary antibodies were detected using AlexaFluor568 goat anti-mouse (1:200, Invitrogen) and AlexaFluor488 goat anti-rabbit (1:200, Invitrogen) for 1 h at room temperature. To test whether plasmin stimulation leads to cleavage and release of the inhibitory peptide, M-1 cells grown on coverslips were incubated with plasmin for 5 min at room temperature in HBSS, briefly washed, and fixed for 10 min in 4% formaldehyde in PBS. Coverslips were then washed in PBST and then incubated with the γENaC inhibitory peptide-specific monoclonal antibody and rabbit polyclonal γENaC antibody (Sigma) for 1 h at room temperature. After incubation, the coverslips were washed in PBST, and nucleic acid was visualized using DAPI (Invitrogen). Actin was stained using Atto488-phalloidin (Sigma). Images were acquired as stacks of images with confocal laser-scanning microscopy (Olympus FV1000) using a ×20 (numerical aperture, 0.5) Olympus water immersion objective. The scanning area was set to 800 × 800 or 1,024 × 1,024 pixels with and without internal zoom. DAPI, AlexaFluor488, and AlexaFluor568 were sequentially excited using 405-nm, 488-nm, and 559-nm lasers, respectively, and fluorescence was monitored through appropriate filter settings (AOTF). The fluo-

Downloaded from http://ajpregu.physiology.org/ by 10.220.33.1 on January 14, 2017

rescence signal from the monoclonal antibody was enhanced post hoc using Adobe Photoshop CS4. Colocalization was calculated using the Pearson-Spearman correlation colocalization plug-in (15) (http://www.cpib.ac.uk/~afrench/coloc.html) for Image J (version 1.40g, http://rsb.info.nih.gov/ij/). The images are shown as maximum intensity projections of stacks of 12–15 images.

Immunoblotting. M-1 cells were lysed in ice-cold Tris-EDTA buffer [0.1 M Tris, 10 mM EDTA, 1 mM DTT, 1% Triton X-100, pH 7.2] containing Complete protease inhibitor (Roche, Hvidovre, Denmark), and 10× reducing agent (Invitrogen) and 4× LDS sample buffer (Invitrogen) was added. After boiling, the samples were subjected to SDS-PAGE (Bio-Rad) and subsequently transferred to a PVDF membrane (Immobilon-P, Millipore, Copenhagen, Denmark). Blots were probed with monoclonal mouse anti-human prostasin (BD Biosciences, Brondby Denmark) or polyclonal rabbit anti-actin (Abcam, Cambridge, MA). Primary antibodies were detected with HRP-coupled antibodies (Dako, Glostrup, Denmark) and enhanced chemiluminescence system (Amersham Biosciences).

Statistics. Results are presented as mean ± SE, and *n* is the number of observations. SigmaPlot 9.0 (Systat Software, Chicago, IL) was used for data analysis and data fitting. $P < 0.05$ was considered significant.

RESULTS

Plasmin interacts with prostasin. Cy3-labeled plasmin was employed to elucidate whether plasmin binds to the cell surface of the mouse renal cortical collecting duct cell line, M-1. In superfusion experiments, 10 μg/ml of Cy3-labeled plasmin rapidly binds to the surface of live M-1 cells (see Fig. 1*A* and Supplemental Video 1 in the online version of this article). To identify the interaction partner of plasmin, biotin-label transfer was used. After stimulation of M-1 cells with plasmin conjugated to a biotin-labeled cross-linker, biotin-tagged proteins were precipitated using streptavidin and subjected to immunoblotting. Fig. 1*B* shows an immunoblot against biotinylated proteins after biotin transfer. In the lanes using plasmin concentrations of 20–40 μg, a significant band at ~40 kDa was detected. When the ENaC-activating serine protease trypsin

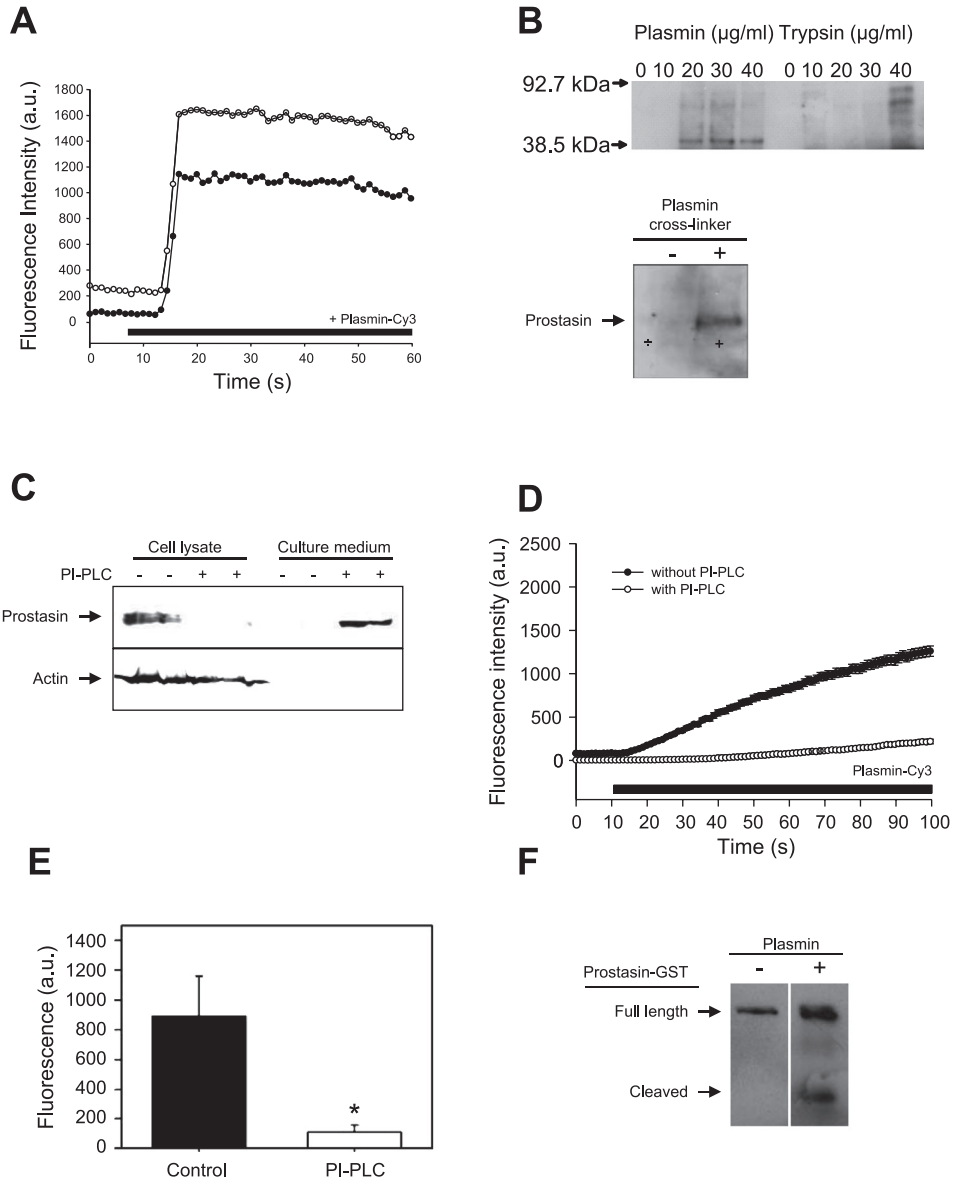

Fig. 1. Plasmin interacts with prostasin. *A*: fluorescence traces were obtained in M-1 cells that were superfused with Cy3-coupled plasmin (10 μg/ml), and emitted fluorescence was recorded by confocal microscopy. After the addition of Cy3-coupled plasmin, the fluorescence intensity increases rapidly, indicating that plasmin binds M-1 cells. Solid and open circles represent cell numbers 1 and 2, respectively, which can be seen live in Supplemental Video 1 in the online version of this article. *B, top*: immunoblot shows precipitate from streptavidin precipitation of M-1 cells after crosslinking with plasmin (10–40 μg/ml) and trypsin (10–40 μg/ml). It can be seen that plasmin interacts with a ~40-kDa protein, and trypsin interacts with several molecules between 50 and 90 kDa. *Bottom*: Western blot shows that the 40-kDa plasmin-interacting protein reacts with a specific antibody directed against prostasin ($n = 3$). *C*: monolayers of M-1 cells were treated with PI-PLC (0.1 U/ml) added to the medium. After incubation, cell-conditioned medium and cell lysate were harvested and used for Western blotting for prostasin. PI-PLC treatment reduces the prostasin level in the cell lysate and increases the prostasin level in the culture medium. *D*: fluorescence traces from M-1 cells that preincubated with PI-PLC before treatment with Cy3-labeled plasmin. The traces show that PI-PLC treatment of the cells leads to a reduced fluorescence signal, i.e., less binding of plasmin, compared with control cells after superfusion with Cy3-plasmin (1 μg/ml, $n = 30$ cells). *E*: bar graph depicts the average emitted fluorescence ± SE from M-1 cells treated with or without PI-PLC and subsequently superfused with Cy3-plasmin ($n = 3$). *$P < 0.05$. *F*: immunoblot of GST-tagged prostasin probed with a specific prostasin antibody. GST-tagged prostasin was incubated with or without plasmin. Incubation with plasmin leads to cleavage of GST-tagged prostasin in vitro.

Downloaded from http://ajpregu.physiology.org/ by 10.220.33.1 on January 14, 2017

was used for biotin-label transfer, several bands ranging from 50 to 90 kDa appeared on the blots, but the band at 40 kDa was not detectable. Further immunoblot analysis identified the ~40-kDa band as prostasin (Fig. 1*B*), which is a GPI-anchored ENaC activating serine protease (1, 9, 42). To assess the importance of the GPI anchor for the binding of plasmin to M-1 cell surfaces, cells were pretreated with phosphatidylinositol-specific phospholipase C (PI-PLC), which cleaves GPI anchors. After incubation with PI-PLC, the level of prostasin in the cell lysate was reduced, whereas the prostasin level in the culture medium increased (Fig. 1*C*). This indicates that prostasin is mainly anchored to the cell surface via a GPI-anchor in M-1 cells. The PI-PLC-treated cells showed a reduced binding of 1 μg/ml Cy3-labeled plasmin compared with control cells, indicating that a GPI-anchored protein is involved in the binding (Fig. 1, *D* and *E*). Prostasin is synthesized as an inactive zymogen that is activated by a single endoproteolytic cleavage. The activation of prostasin has been shown to occur at the plasma membrane (32). Using recombinant prostasin with a C-terminal GST-tag, we tested whether plasmin could cleave prostasin. After prostasin incubated with plasmin, two bands appeared, with the estimated size of full-length prostasin and prostasin cleaved at the activation site (Fig. 1*F*). Next, site-specific siRNA-mediated knockdown of prostasin expression in M-1 cells was used to examine binding of labeled plasmin. In a concentration-response experiment, transfection of M-1 cells with prostasin siRNA led to a concentration-dependent decrease in prostasin mRNA level (Fig. 2*A*). A maximal prostasin mRNA knockdown was achieved at a siRNA concentration of 50 nM. This concentration also led to knockdown of prostasin at the protein level (Fig. 2*A*, *right*) and was used in subsequent experiments. Prostasin knockdown significantly attenuated binding of Cy3-labeled plasmin to M-1 cells (Fig. 2*B*). Thus, the data suggest that plasmin interacts with and activates prostasin on the cell surface of M-1 cells.

Involvement of prostasin in plasmin-stimulated ENaC activity. We next investigated whether prostasin was functionally involved in plasmin-stimulated ENaC activity. To test whether a GPI-anchored protein is involved in plasmin-stimulated ENaC activity, monolayers of M-1 cells were treated with or without PI-PLC before measuring the short-circuit currents in response to different plasmin concentrations. The PI-PLC-treated monolayers showed a reduced plasmin-stimulated current compared with control monolayers at plasmin concentrations of 1.3 to 3.90 μg/ml (Fig. 3*A*). However, there was no difference between monolayers treated with or without PI-PLC when using the high plasmin concentration (30 μg/ml) (Fig. 3*A*). Moreover, no differences in baseline, trypsin, and amiloride-insensitive short-circuit currents in monolayers treated with or without PI-PLC were detected (Fig. 3*B*). These data indicate that at least in the range of plasmin concentrations between 1–4 μg/ml, a GPI-anchored protein is necessary for the plasmin-stimulated ENaC activity, while at higher concentrations a direct interaction with ENaC is more likely.

The functional significance of prostasin knockdown was tested using the whole-cell configuration of the patch-clamp technique. Single M-1 cells transfected with control siRNA (50 nmol/l) showed a significant increase in whole-cell current after stimulation with plasmin (10 μg/ml) or nephrotic urine (Fig. 3, *C* and *D*), which we previously have shown to be mediated by ENaC (41). However, siRNA-mediated knockdown of prostasin blocked the ability of plasmin (10 μg/ml) and nephrotic rat urine to stimulate ENaC current in M-1 cells (Fig. 3, *C* and *D*). This suggests that prostasin is involved in plasmin-stimulated ENaC activity.

Prostasin and γENaC are colocalized in M-1 cells. Attempts to detect endogenous prostasin using immunofluorescence were unsuccessful, and therefore, we expressed human prostasin with a C-terminal FLAG-tag in M-1 cells. We found that

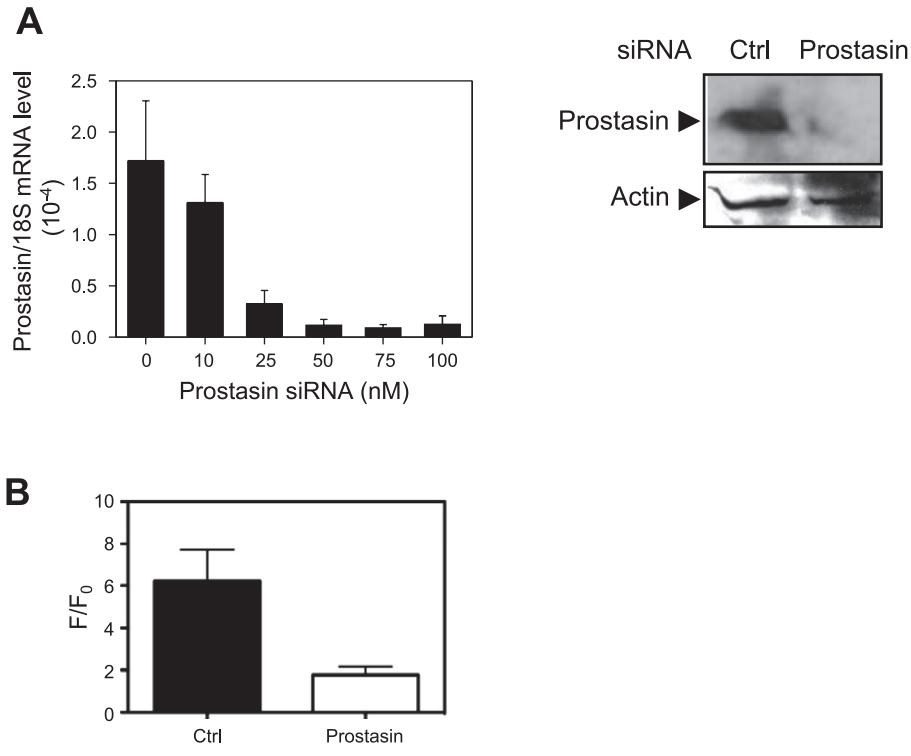

Fig. 2. *A*: bar graph shows the effect of transfection of M-1 cells with increasing concentrations of specific siRNAs directed against prostasin on the abundance of prostasin mRNA (means ± SE). Cells were transfected with prostasin siRNAs, and prostasin mRNA levels were assessed the following day using quantitative RT-PCR ($n = 4$). Prostasin protein abundance was determined by Western blot analysis of M-1 cell protein homogenates 2 days after siRNA transfection (50 nmol/l). *Right*: result of blots for prostasin (*top*) and β-actin (*lower*). *B*: bar graph shows the effect of siRNA-mediated (50 nmol/l) knockdown of prostasin on binding of Cy3-labeled plasmin to M-1 cells, as determined by confocal microscopy ($n = 6$). *F*: cell fluorescence at the end of the experiment; F_0: fluorescence at the start of experiment.

Downloaded from http://ajpregu.physiology.org/ by 10.220.33.1 on January 14, 2017

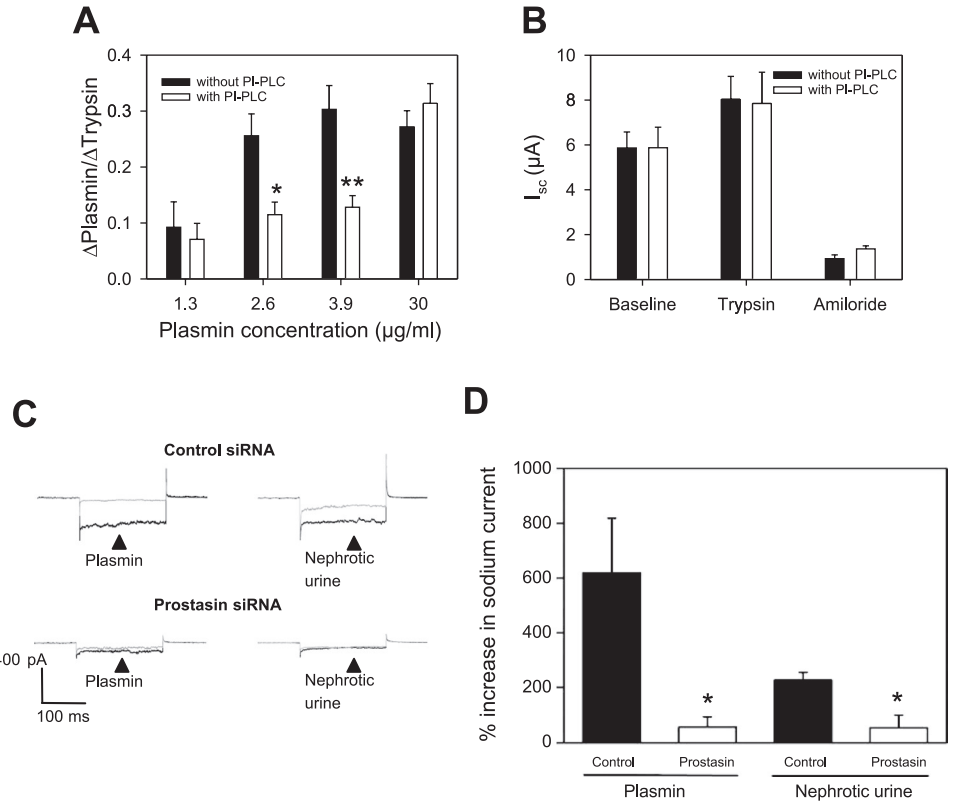

Fig. 3. Effect of GPI-anchored prostasin on plasmin-stimulated ENaC currents in M-1 cells. *A*: average ratio between plasmin-activated (ΔPlasmin) and trypsin-activated (ΔTrypsin) short-circuit currents from M-1 cell monolayers grown on permeable filters and mounted in Ussing chambers. First, M-1 cells were treated with or without phospholipase C (PI-PLC) to disrupt GPI anchors. Next, the short-circuit current response to different plasmin concentrations was evaluated (ΔPlasmin). Subsequently, trypsin was added, and the trypsin-induced current (ΔTrypsin) was used to normalize the plasmin-induced current (ΔPlasmin/ΔTrypsin). Plasmin-evoked currents were larger in M-1 cells not pretreated with PI-PLC in a low concentration range of plasmin, whereas at higher concentrations of plasmin, the PI-PLC treatment did not attenuate the current. This suggests involvement of a GPI-anchored protein in the response to plasmin at concentrations below 10 μg/ml. $*P < 0.05$, $**P < 0.01$. *B*: short-circuit current from M-1 cell monolayers mounted in Ussing chambers and pretreated with PI-PLC or vehicle. Trypsin enhanced significantly short-circuit current independent of PI-PLC pretreatment, and this was abolished by the addition of amiloride ($n = 5$). *C*: original current traces in response to a step depolarization obtained in single M-1 cells by patch-clamp recordings. M-1 cells were mock transfected (control siRNA) or transfected with prostasin siRNA 2 days before the experiments. Gray traces are from cells before superfusion with pure plasmin (10 μg/ml) or urine from rats with proteinuria (PAN nephrosis), and black traces are from same cells after superfusion with plasmin or rat urine. *D*: bar graph shows the average changes in current obtained in patch-clamp experiments with single M-1 cells in response to plasmin (10 μg/ml) and nephrotic urine. Pretreatment with prostasin siRNAs significantly attenuated plasmin- and nephrotic urine-evoked currents in M-1 cells. ($n = 4$), $*P < 0.05$.

immunofluorescence images of M-1 cells transfected with FLAG-tagged prostasin showed colocalization of prostasin and γENaC (Pearson coefficient 0.74 and Spearman coefficient 0.59), in contrast to mock-transfected cells in which no prostasin labeling was detected (see Supplemental Fig. 1 in the online version of this article). We used the Duolink in situ proximity ligation assay (40) to corroborate the colocalization of prostasin and γENaC. Using primary antibodies from two different species, e.g., rabbit anti-γENaC directed against the nonprocessed cytoplasmic part and mouse anti-FLAG, this assay is capable of reporting whether proteins are in close proximity (<40 nm) of each other, which is indicated by bright red fluorescent spots. In a subset of M-1 cells expressing the FLAG-tagged prostasin, a punctuated fluorescent signal was observed that indicates that prostasin and γENaC are separated by less than 40 nm (Fig. 4*A*). Because cells were permeabilized, it is not possible to determine whether colocalization is confined to the cell surface. Cells not expressing the FLAG-tagged prostasin and omission of the γENaC antibody abolished this labeling pattern (not shown). Thus, these data indicate that prostasin and γENaC are colocalized in M-1 cells.

Plasmin induces prostasin-dependent release of γENaC inhibitory peptide. We (41) and others (35) have previously shown that plasmin induces cleavage of γENaC. To test whether prostasin is involved in the plasmin-induced cleavage of γENaC, we generated a monoclonal antibody directed against the N-terminal part of the proposed inhibitory peptide. The antibody yielded no labeling of mock-transfected human embryonic kidney cells but produced marked labeling af M-1 cells transfected with γENaC expression vector (see Supplemental Fig. 2 in the online version of this article). Immunoblotting showed that the antibody yielded two prominent bands in native M1 plasma membrane fractions. Two products exhibited molecular size around 100 kDa and one was below 75 kDa (Supplemental Fig. 2). Using confocal laser-scanning microscopy, we found that the antibody yielded specific labeling that was associated with M-1 cells and that preabsorption of the antibody with 10 μg/ml of the immunogenic peptide abolished the labeling (Fig. 4*B*). Pretreatment of the cells with 10 μg/ml plasmin for 5 min abolished labeling, which indicates that plasmin releases the γENaC inhibitory peptide (Fig. 4*B*). Compared with cells transfected with negative control siRNA, cells transfected with prostasin siRNA displayed a stronger immuno-

Downloaded from http://ajpregu.physiology.org/ by 10.220.33.1 on January 14, 2017

fluorescence labeling with the antibody after pretreatment with 5–10 μg/ml plasmin (Fig. 4*C*). However, there was no difference detected in the labeling pattern between M-1 cells transfected with negative control and prostasin siRNA after pretreatment with 30 μg/ml plasmin siRNA (Fig. 4*C*). These data suggest that at low plasmin concentration, prostasin is involved in the cleavage of the γENaC subunit.

DISCUSSION

We have recently shown that plasminogen is filtered across the glomerular barrier in a rat model of nephrotic syndrome and subsequently activated to plasmin by urokinase-type plasminogen activator in the renal tubular system (41). Pure plasmin and nephrotic urine, which contains active plasmin, acti-

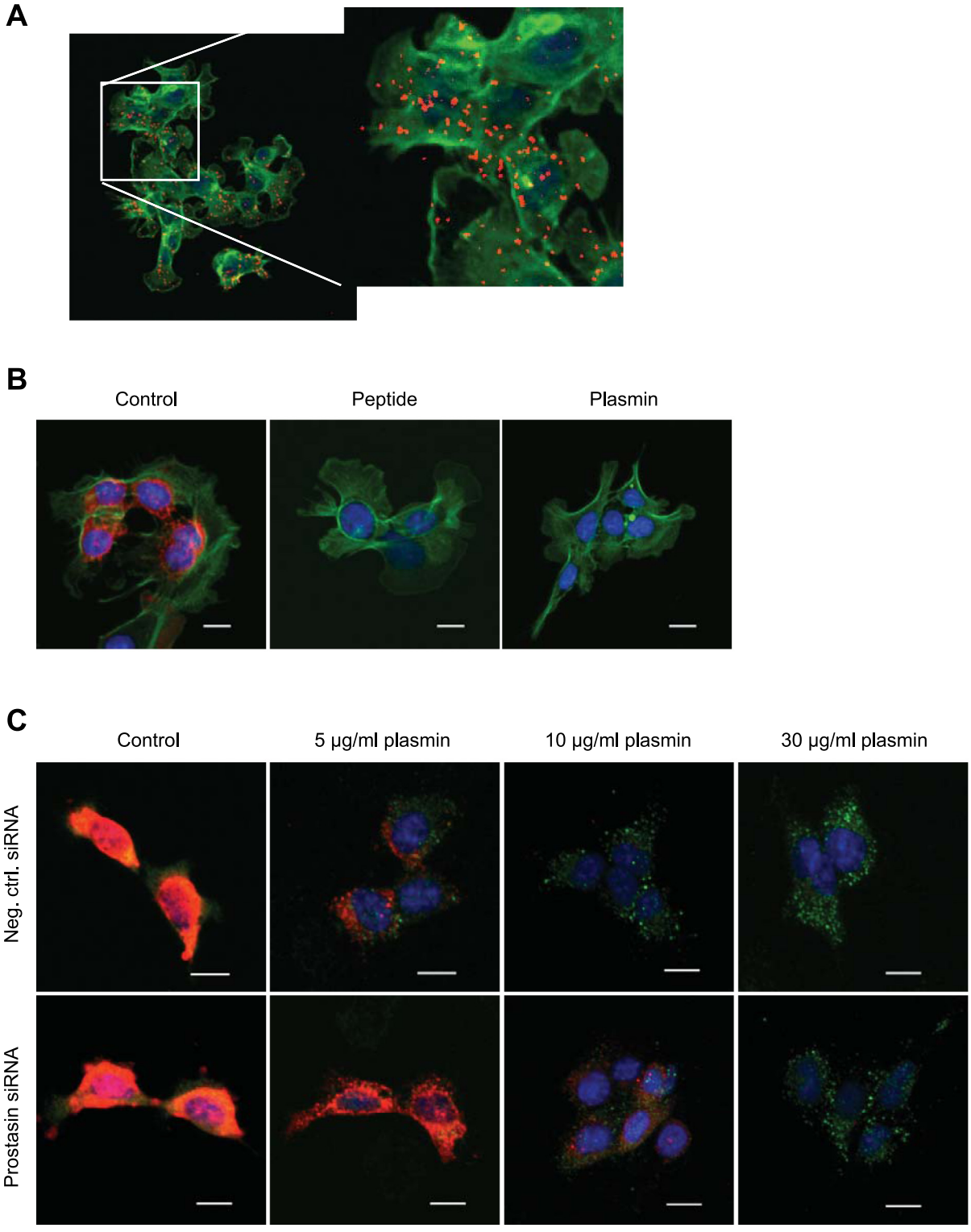

Downloaded from http://ajpregu.physiology.org/ by 10.220.33.1 on January 14, 2017

vate ENaC by proteolytic modification of the γ subunit (35, 41). The present study was undertaken to investigate the mechanism by which plasmin stimulates ENaC activity. Our data show that pure plasmin binds to GPI-anchored prostasin on the surface of M-1 cells and that plasmin treatment of tagged prostasin results in the appearance of a cleavage product, which is compatible with proteolytic modification. Prostasin subsequently cleaves the γ subunit of ENaC, leading to the release of an inhibitory peptide from the extracellular domain and activation of the channel. The effect of plasmin was concentration dependent, and in the high range of tested concentrations, plasmin activated ENaC directly.

It is well known that cascades of sequential activation of serine proteases drive processes, such as blood coagulation, complement fixation, and fibrinolysis (20). Prostasin is a downstream target in a proteolytic cascade that involves matriptase in a process regulating terminal epidermal differentiation (27, 32). However, the finding that plasmin-stimulated ENaC activity involves a serine protease cascade with prostasin is novel. Our data cannot rule out that a serial proteolytic action of prostasin and plasmin on γENaC is responsible for the observed effect. However, ENaC is fully activated by furin- and prostasin-dependent release of the inhibitory peptide from the γ subunit (4), and the proposed cleavage sites for prostasin and plasmin (at high concentrations) are located adjacent to each other (35). Thus, a mechanism involving sequential prostasin- and plasmin-dependent γENaC cleavage seems less likely. Because prostasin is expressed in collecting ducts in vivo (46), this observation may be relevant to understand the pathophysiological ENaC-dependent NaCl retention associated with proteinuric diseases such as nephrotic syndrome (41) and anti-Thy1 glomerulonephritis (17). Proteolytic processing of ENaC blunts Na^+ self-inhibition (10, 39) by releasing the inhibitory peptide form the γ-subunit. The inhibitory peptide is flanked by cleavage sites for furin, on one side, and prostasin and plasmin (at a high concentration) on the other.

The set of data indicates that plasmin interacts with GPI-anchored prostasin. In agreement with previous observations (9), we found that the major pool of endogenously expressed prostasin in M-1 cells was GPI-anchored. In the low range of the tested plasmin concentrations (below 10 μg/ml), we found that intact GPI-anchored proteins and prostasin expression were necessary for stimulation of ENaC, whereas at higher concentrations, the plasmin-stimulation was independent of GPI-anchored proteins. GPI-anchored proteins are mainly located in microdomains termed lipid rafts (38), which have also been shown to contain endogenous ENaC (21). This is in agreement with our finding that prostasin and γENaC are colocalized. The anchoring of prostasin in lipid rafts appears to be important for its ENaC-activating function, since mutation of the GPI-anchored motif in prostasin leaves it unable to activate ENaC (44). Thus, at low plasmin concentration, lipid rafts could provide an environment, which favors the plasmin-stimulated ENaC activity through prostasin. Passero et al. (35) have observed an additional ENaC cleavage product when using plasmin at a high concentration (27 μg/ml), which could be abolished by mutating a site (γK194A) distal to the prostasin cleavage site. This is in agreement with our data and suggests that at high concentrations, plasmin interacts and cleaves γENaC directly. Similar to this observation, trypsin-stimulated ENaC activity was not dependent on prostasin. In accord, trypsin interacted with several molecules in M-1 cells larger than prostasin, with a size that ranged from 50 to 90 kDa. The two prominent trypsin-interacting molecules of sizes around 80 and 90 kDa might be speculated to be the γ subunit of ENaC (19). Although the present data show that prostasin is involved in plasmin-stimulated ENaC activation, we cannot rule out that there exist further intermediate steps between prostasin and ENaC and other techniques with higher spatial resolution, e.g., fluorescence resonance energy transfer, should be used to resolve this issue.

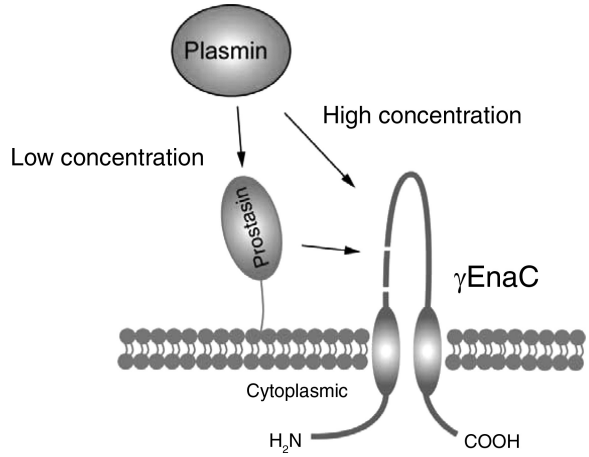

Fig. 5. Proposed model for plasmin-stimulated ENaC activity. At low concentration, plasmin interacts with GPI-anchored prostasin at the cell surface, which subsequently leads to cleavages of the γ subunit of ENaC and release of the inhibitory peptide. At high concentrations, plasmin-stimulated ENaC activity does not appear to involve prostasin but occurs through direct cleavage of the subunit.

Fig. 4. Stimulation of M-1 cells with plasmin leads to prostasin-dependent cleavage of γENaC. *A*: Duolink in situ proximity ligation assay was used to test the hypothesis that prostasin and γENaC are closely adjacent in M-1 cells. The immunocytofluorescence labeling shows that prostasin and γENaC are separated by less than 40 nm (bright red spots) in M-1 cells expressing FLAG-tagged prostasin. Cytoplasmic actin was visualized with phalloidin-Atto488 (green), and cell nuclei were visualized with DAPI (blue). *Right*: magnification of the boxed area. Red signal intensity was increased post hoc. *B:* immunofluorescence labeling of M-1 cells with a specific antibody directed against the inhibitory peptide segment of the γENaC extracellular domain (red fluorescence signal). Labeling is associated with control M-1 cells (red). Nuclei are stained blue with DAPI. Labeling is abolished by preabsorption of the antibody with the immunogenic peptide (*middle*) and prevented after pretreatment of M-1 cells with 10 μg/ml plasmin for 5 min (*right*). Blue staining denotes DAPI staining. Green staining denotes labeling of actin cytoskeleton with phalloidin-Atto488. Scale bar = 10 μm. *C*: immunofluorescence labeling of M-1 cells with specific antibodies directed against the inhibitory peptide-segment within the extracellular domain of γENaC (red fluorescence) and a region of γENaC, which is not proteolytically modified (green fluorescence). M-1 cells were pretreated with siRNA directed against prostasin (*bottom*) or negative control siRNA (*top*). Before immunofluorescensce labeling, prostasin-siRNA-treated and control siRNA-treated cells incubated with increasing concentrations of plasmin. Plasmin concentration dependently prevented labeling for the inhibitory γENaC-peptide in M-1 cells treated with control siRNA (*top*). In M-1 cells treated with siRNA directed against prostasin, plasmin had a reduced ability to prevent labeling for the inhibitory γENaC-peptide (red signal), whereas labeling for a region of γENaC, which is not proteolytically modified (green signal) was not altered (*bottom*). Blue staining of cell nuclei with DAPI. Green staining denotes cytoplasmic epitope of γENaC. Red denotes inhibitory peptide of γENaC extracellular domain. Red signal intensity was amplified post hoc in this photo. Scale bar: 10 μm.

Downloaded from http://ajpregu.physiology.org/ by 10.220.33.1 on January 14, 2017

The (patho)physiological consequences of these findings remain elusive at present. Recently, we have shown that plasmin in nephrotic urine from humans and rats activates ENaC (41). On the basis of a serine protease activity assay, we have estimated a plasmin concentration of 10–15 μg/ml in urine from puromycin aminonucleoside-induced nephrotic syndrome in rats at the peak of proteinuria (data not shown). Thus, the prostasin-dependent step in plasmin-stimulated ENaC activity would probably play a minor role in sodium retention at the peak of proteinuria. However, human nephrotic urine displayed a much lower serine protease activity compared with rat urine from the PAN nephrotic model (41), suggesting that ENaC activation and sodium retention in nephrotic patients could be prostasin-dependent. Moreover, the proteinuria in nephrotic patients is at the extreme of the spectrum, and most clinical proteinuric conditions exhibit a lower degree of proteinuria.

Recent data show that the γ subunit of ENaC exists at the cell surface with smaller molecular size than full-length subunits, depending on SGK1 and sodium status (14), such that Na-depletion increases the cleaved form several times at the membrane surface (16). A recent study showed that γENaC subunit appears to be proteolytic processed in proteinuric glomerulonephritis (17). Thus, proteolytic modification of γENaC appears to occur under physiological and pathophysiological conditions. The dominance of cleaved γENaC at the cell surface in sodium-depleted states is consistent with the observation that prostasin expression is stimulated by aldosterone (31, 33). Intriguingly, camostat mesilate has been shown to be an inhibitor of prostasin activity (12, 29) that reduced blood pressure and renal injury in salt-sensitive rats (29). In patients with advanced diabetic nephropathy camostat reduced edema volume (25). Although indirect, these data are in accord with a role of prostasin to promote sodium retention in vivo.

Perspectives and Significance

The present study provides evidence that plasmin-stimulated ENaC activity depends on GPI-anchored prostasin at low plasmin concentration, whereas the activation is prostasin independent at high plasmin concentrations (Fig. 5). The study identifies prostasin as a potential drug target in diseases with proteinuria and abnormal activation of ENaC.

Nephrotic syndrome is at one extreme of an array of proteinuric conditions. Several human diseases, e.g., other primary kidney disease, diabetes mellitus, hypertension, and preeclampsia are characterized by microalbuminuria (or proteinuria) and sodium retention. Thus, it is of interest to establish whether tubular formation of prostasin-dependent plasmin-stimulated ENaC activation may contribute to sodium retention in these conditions.

ACKNOWLEDGMENTS

We thank Drs. Ulla G. Friis and Finn Jørgensen for expert help and advice with the electrophysiological techniques, as well as Lars Vitved for skillfull technical assistance in the production of the monoclonal antibody.

GRANTS

This work was supported by the Danish Medical Research Council, the NOVO Nordisk Foundation, Helen and Ejnar Bjørnows Foundation, and the Lundbeck Foundation.

DISCLOSURES

No conflicts of interest are declared by the authors.

REFERENCES

1. **Adachi M, Kitamura K, Miyoshi T, Narikiyo T, Iwashita K, Shiraishi N, Nonoguchi H, Tomita K.** Activation of epithelial sodium channels by prostasin in Xenopus oocytes. *J Am Soc Nephrol* 12: 1114–1121, 2001.
2. **Alvarez dlR, Li H, Canessa CM.** Effects of aldosterone on biosynthesis, traffic, and functional expression of epithelial sodium channels in A6 cells. *J Gen Physiol* 119: 427–442, 2002.
3. **Bistrup C, Thiesson HC, Jensen BL, Skott O.** Reduced activity of 11β-hydroxysteroid dehydrogenase type 2 is not responsible for sodium retention in nephrotic rats. *Acta Physiol Scand* 184: 161–169, 2005.
4. **Bruns JB, Carattino MD, Sheng S, Maarouf AB, Weisz OA, Pilewski JM, Hughey RP, Kleyman TR.** Epithelial Na^+ channels are fully activated by furin- and prostasin-dependent release of an inhibitory peptide from the gamma subunit. *J Biol Chem* 282: 6153–6160, 2007.
5. **Bruns JB, Carattino MD, Sheng S, Maarouf AB, Weisz OA, Pilewski JM, Hughey RP, Kleyman TR.** Epithelial Na^+ channels are fully activated by furin- and prostasin-dependent release of an inhibitory peptide from the gamma-subunit. *J Biol Chem* 282: 6153–6160, 2007.
6. **Caldwell RA, Boucher RC, Stutts MJ.** Neutrophil elastase activates near-silent epithelial Na^+ channels and increases airway epithelial Na^+ transport. *Am J Physiol Lung Cell Mol Physiol* 288: L813–L819, 2005.
7. **Caldwell RA, Boucher RC, Stutts MJ.** Serine protease activation of near-silent epithelial Na^+ channels. *Am J Physiol Cell Physiol* 286: C190–C194, 2004.
8. **Canessa CM, Schild L, Buell G, Thorens B, Gautschi I, Horisberger JD, Rossier BC.** Amiloride-sensitive epithelial Na^+ channel is made of three homologous subunits. *Nature* 367: 463–467, 1994.
9. **Chen LM, Skinner ML, Kauffman SW, Chao J, Chao L, Thaler CD, Chai KX.** Prostasin is a glycosylphosphatidylinositol-anchored active serine protease. *J Biol Chem* 276: 21434–21442, 2001.
10. **Chraibi A, Horisberger JD.** Na self-inhibition of human epithelial Na channel: temperature dependence and effect of extracellular proteases. *J Gen Physiol* 120: 133–145, 2002.
11. **Chraibi A, Vallet V, Firsov D, Hess SK, Horisberger JD.** Protease modulation of the activity of the epithelial sodium channel expressed in *Xenopus* oocytes. *J Gen Physiol* 111: 127–138, 1998.
12. **Coote K, Atherton-Watson H, Sugar R, Young A, Mackenzie-Beevor A, Gosling M, Bhalay G, Bloomfield G, Dunstan A, Bridges RJ, Sabater JR, Abraham WM, Tully D, Pacoma R, Schumacher A, Harris JL, Danahay HL.** Camostat attenuates airway ENaC function in vivo through the inhibition of a channel activating protease. *J Pharmacol Exp Ther* 329: 764–774, 2009.
13. **Ecelbarger CA, Kim GH, Terris J, Masilamani S, Mitchell C, Reyes I, Verbalis JG, Knepper MA.** Vasopressin-mediated regulation of epithelial sodium channel abundance in rat kidney. *Am J Physiol Renal Physiol* 279: F46–F53, 2000.
14. **Fejes-Toth G, Frindt G, Naray-Fejes-Toth A, Palmer LG.** Epithelial Na^+ channel activation and processing in mice lacking SGK1. *Am J Physiol Renal Physiol* 294: F1298–F1305, 2008.
15. **French AP, Mills S, Swarup R, Bennett MJ, Pridmore TP.** Colocalization of fluorescent markers in confocal microscope images of plant cells. *Nat Protocols* 3: 619–628, 2008.
16. **Frindt G, Ergonul Z, Palmer LG.** Surface expression of epithelial Na channel protein in rat kidney. *J Gen Physiol* 131: 617–627, 2008.
17. **Gadau J, Peters H, Kastner C, Kuhn H, Nieminen-Kelha M, Khadzhynov D, Kramer S, Castrop H, Bachmann S, Theilig F.** Mechanisms of tubular volume retention in immune-mediated glomerulonephritis. *Kidney Int* 75: 699–710, 2009.
18. **Garty H, Palmer LG.** Epithelial sodium channels: function, structure, and regulation. *Physiol Rev* 77: 359–396, 1997.
19. **Harris M, Firsov D, Vuagniaux G, Stutts MJ, Rossier BC.** A novel neutrophil elastase inhibitor prevents elastase activation and surface cleavage of the epithelial sodium channel expressed in *Xenopus laevis* oocytes. *J Biol Chem* 282: 58–64, 2006.
20. **Hedstrom L.** Serine protease mechanism and specificity. *Chem Rev* 102: 4501–4524, 2002.
21. **Hill WG, An B, Johnson JP.** Endogenously expressed epithelial sodium channel is present in lipid rafts in A6 cells. *J Biol Chem* 277: 33541–33544, 2002.

Downloaded from http://ajpregu.physiology.org/ by 10.220.33.1 on January 14, 2017

22. **Hughey RP, Bruns JB, Kinlough CL, Harkleroad KL, Tong Q, Carattino MD, Johnson JP, Stockand JD, Kleyman TR.** Epithelial sodium channels are activated by furin-dependent proteolysis. *J Biol Chem* 279: 18111–18114, 2004.
23. **Hughey RP, Bruns JB, Kinlough CL, Kleyman TR.** Distinct pools of epithelial sodium channels are expressed at the plasma membrane. *J Biol Chem* 279: 48491–48494, 2004.
24. **Hughey RP, Carattino MD, Kleyman TR.** Role of proteolysis in the activation of epithelial sodium channels. *Curr Opin Nephrol Hypertens* 16: 444–450, 2007.
25. **Ikeda Y, Ito H, Hashimoto K.** Effect of camostat mesilate on urinary protein excretion in three patients with advanced diabetic nephropathy. *J Diabetes Complications* 13: 56–58, 1999.
26. **Kohler G, Milstein C.** Continuous cultures of fused cells secreting antibody of predefined specificity. *Nature* 256: 495–497, 1975.
27. **Leyvraz C, Charles RP, Rubera I, Guitard M, Rotman S, Breiden B, Sandhoff K, Hummler E.** The epidermal barrier function is dependent on the serine protease CAP1/Prss8. *J Cell Biol* 170: 487–496, 2005.
28. **Loffing J, Zecevic M, Feraille E, Kaissling B, Asher C, Rossier BC, Firestone GL, Pearce D, Verrey F.** Aldosterone induces rapid apical translocation of ENaC in early portion of renal collecting system: possible role of SGK. *Am J Physiol Renal Physiol* 280: F675–F682, 2001.
29. **Maekawa A, Kakizoe Y, Miyoshi T, Wakida N, Ko T, Shiraishi N, Adachi M, Tomita K, Kitamura K.** Camostat mesilate inhibits prostasin activity and reduces blood pressure and renal injury in salt-sensitive hypertension. *J Hypertens* 27: 181–189, 2009.
30. **Masilamani S, Kim GH, Mitchell C, Wade JB, Knepper MA.** Aldosterone-mediated regulation of ENaC alpha, beta, and gamma subunit proteins in rat kidney. *J Clin Invest* 104: R19–R23, 1999.
31. **Narikiyo T, Kitamura K, Adachi M, Miyoshi T, Iwashita K, Shiraishi N, Nonoguchi H, Chen LM, Chai KX, Chao J, Tomita K.** Regulation of prostasin by aldosterone in the kidney. *J Clin Invest* 109: 401–408, 2002.
32. **Netzel-Arnett S, Currie BM, Szabo R, Lin CY, Chen LM, Chai KX, Antalis TM, Bugge TH, List K.** Evidence for a matriptase-prostasin proteolytic cascade regulating terminal epidermal differentiation. *J Biol Chem* 281: 32941–32945, 2006.
33. **Olivieri O, Castagna A, Guarini P, Chiecchi L, Sabaini G, Pizzolo F, Corrocher R, Righetti PG.** Urinary prostasin: a candidate marker of epithelial sodium channel activation in humans. *Hypertension* 46: 683–688, 2005.
34. **Palmer LG, Garty H, Selden DW, Giebisch G.** Epithelial Na channels. In: *The Kidney: Physiology and Pathophysiology*. New York: Lippincott Williams & Wilkins, 2000, p. 251–276.
35. **Passero CJ, Mueller GM, Rondon-Berrios H, Tofovic SP, Hughey RP, Kleyman TR.** Plasmin activates epithelial Na^+ channels by cleaving the gamma subunit. *J Biol Chem* 283: 36586–36591, 2008.
36. **Planes C, Caughey GH.** Regulation of the epithelial Na^+ channel by peptidases. *Curr Top Dev Biol* 78: 23–46, 2007.
37. **Rossier BC, Stutts MJ.** Activation of the epithelial sodium channel (ENaC) by serine proteases. *Annu Rev Physiol* 71: 361–379, 2009.
38. **Sharom FJ, Lehto MT.** Glycosylphosphatidylinositol-anchored proteins: structure, function, and cleavage by phosphatidylinositol-specific phospholipase C. *Biochem Cell Biol* 80: 535–549, 2002.
39. **Sheng S, Carattino MD, Bruns JB, Hughey RP, Kleyman TR.** Furin cleavage activates the epithelial Na^+ channel by relieving Na^+ self-inhibition. *Am J Physiol Renal Physiol* 290: F1488–F1496, 2006.
40. **Soderberg O, Gullberg M, Jarvius M, Ridderstrale K, Leuchowius KJ, Jarvius J, Wester K, Hydbring P, Bahram F, Larsson LG, Landegren U.** Direct observation of individual endogenous protein complexes in situ by proximity ligation. *Nat Methods* 3: 995–1000, 2006.
41. **Svenningsen P, Bistrup C, Friis UG, Bertog M, Haerteis S, Krueger B, Stubbe J, Jensen ON, Thiesson HC, Uhrenholt TR, Jespersen B, Jensen BL, Korbmacher C, Skott O.** Plasmin in nephrotic urine activates the epithelial sodium channel. *J Am Soc Nephrol* 20: 299–310, 2009.
42. **Vallet V, Chraibi A, Gaeggeler HP, Horisberger JD, Rossier BC.** An epithelial serine protease activates the amiloride-sensitive sodium channel. *Nature* 389: 607–610, 1997.
43. **Vallet V, Horisberger JD, Rossier BC.** Epithelial sodium channel regulatory proteins identified by functional expression cloning. *Kidney Int Suppl* 67: S109–S114, 1998.
44. **Vallet V, Pfister C, Loffing J, Rossier BC.** Cell-surface expression of the channel activating protease xCAP-1 is required for activation of ENaC in the *Xenopus* oocyte. *J Am Soc Nephrol* 13: 588–594, 2002.
45. **Verrey F, Hummler E, Schild L, Rossier BC, Sheng S, Giebisch G.** Control of Na^+ transport by aldosterone. In: *The Kidney: Physiology and Pathophysiology*. New York: Lippincott Williams & Wilkins, 2000, p. 1441–1471.
46. **Vuagniaux G, Vallet V, Jaeger NF, Pfister C, Bens M, Farman N, Courtois-Coutry N, Vandewalle A, Rossier BC, Hummler E.** Activation of the amiloride-sensitive epithelial sodium channel by the serine protease mCAP1 expressed in a mouse cortical collecting duct cell line. *J Am Soc Nephrol* 11: 828–834, 2000.

Downloaded from http://ajpregu.physiology.org/ by 10.220.33.1 on January 14, 2017